UDC 621.315.592

Experimental and theoretical studies of the influence of anisotropy on the vibrational and electronic properties of α-GeTe

© V.Yu. Davydov, D.A. Pshenay-Severin, A.V. Myasoedov, A.N. Smirnov, I.A. Eliseyev, M.K. Sakhno, A.A. Shabaldin, A.T. Burkov

Ioffe Institute,
194021 St. Petersburg, Russia

E-mail: valery.davydov@mail.ioffe.ru

Received May 5, 2026
Revised June 26, 2026
Accepted June 26, 2026

Using micro-Raman spectroscopy and first-principles calculations, it was shown that the analysis of the angular dependence of the phonon mode intensity in Raman spectra can be used as a non-destructive method for determining crystallographic directions in α-GeTe samples. Strong anisotropy of interband photoluminescence ($\sim 0.7-0.8$ eV) of α-GeTe near the L point of the Brillouin zone was detected for the first time. It was found that at $T = 5$ K, the intensity of the photoluminescence polarized parallel to the trigonal axis is ~ 3 times higher than the intensity of the photoluminescence polarized perpendicular to the axis.

Keywords: germanium telluride, Raman scattering, photoluminescence, density functional theory calculations.

DOI: 10.61011/SC.2026.05.63988.9591

Germanium telluride (GeTe) is a narrow-band-gap semiconductor used in a wide range of devices, including infrared (IR) and ionizing-radiation detectors, laser diodes, and optical recording and data storage devices [1]. GeTe is also the basis of some of the most efficient materials for thermoelectric generators that convert heat into electricity [2,3]. Despite its broad range of applications, however, many of its physical properties remain insufficiently understood. Crystal structure anisotropy plays an important role in determining the optical, electrical, and thermal properties of condensed matter. GeTe is a low-symmetry layered material with strong structural anisotropy, yet studies of the influence of anisotropy on its physical properties are scarce [4,5]. Here we present experimental and theoretical results on the effect of structural anisotropy on the vibrational and electronic properties of GeTe in its rhombohedral modification (α-GeTe).

Bulk GeTe crystals were grown by vapor transport in an evacuated quartz ampoule at 923 K for 170 h. Structural and phase analyses were performed by transmission electron microscopy (TEM) using a JEM JEOL 2100F microscope (Japan) at an accelerating voltage of 200 kV. The vibrational and electronic characteristics of the crystals were measured by micro-Raman spectroscopy (μ-RS) and micro-photoluminescence (μ-PL) using a LabRAM HREvo UV-VIS-NIR-Open spectrometer (Horiba, France) equipped with a confocal microscope and an RC-102 closed-cycle cryostat (Cryo Inc., USA). The $\lambda = 532$ nm (2.33 eV) line of an Nd:YAG laser excited the μ-RS and μ-PL spectra over the temperature range $5-300$ K. The excitation power density was $1-50$ kW/cm^2. The vibrational and electronic structures of bulk α-GeTe were calculated using the Kohn–Sham density functional theory.

The crystal lattice symmetry of α-GeTe is described by space group $R3m$ (№ 160) of the trigonal crystal system (point group C_{3v}). The primitive rhombohedral cell contains one Ge atom and one Te atom. According to standard group-theoretical analysis, the optical phonon spectrum of α-GeTe at the Γ point of the Brillouin zone (BZ) contains two modes of symmetry E and A_1. Both modes are Raman- and IR-active [6]. The Raman tensors for point group C_{3v} are given, for example, in Ref. [7]:

$$R^z_{A_1} = \begin{pmatrix} a & 0 & 0 \\ 0 & a & 0 \\ 0 & 0 & b \end{pmatrix}, \quad R^x_E = \begin{pmatrix} c & 0 & 0 \\ 0 & -c & d \\ 0 & d & 0 \end{pmatrix},$$

$$R^y_E = \begin{pmatrix} 0 & c & d \\ c & 0 & 0 \\ d & 0 & 0 \end{pmatrix}.$$

For the nondegenerate A_1 mode, with atomic displacements polarized along the trigonal axis c_3, the Raman tensor is diagonal and depends on a and b. For the doubly degenerate E mode, polarized in the basal plane (perpendicular to the trigonal axis c_3), the Raman tensor components depend on c and d.

The vibrational anisotropy of α-GeTe was investigated using angle-resolved polarized Raman spectroscopy and first-principles calculations. The Raman tensor components were calculated in Abinit [8,9] using density functional perturbation theory. Since Ge vacancies produce a high hole concentration, the calculations assumed screening of the long-range electric field. The calculated components were $a = 0.19$, $b = 0.27$, $c = 0.11$, and $d = 0.26$ in atomic units.

These Raman tensors were used to calculate the phonon mode intensities in the parallel and crossed polarization components of the Raman spectrum as functions of the incident-light polarization direction for an arbitrary incident beam orientation. Both the E and A_1 modes exhibited characteristic periodic intensity variations whose form depended on the incident beam direction relative to the crystallographic axes.

The angular dependences of the A_1 mode are the simplest: their form is determined solely by the angle between the light wave vector $\mathbf{k}$ and the trigonal axis c_3. The Raman intensities for parallel $I_{A_1}^{VV}(\psi)$ and crossed $I_{A_1}^{VH}(\psi)$ polarizations are given by

$$I_{A_1}^{VV} \sim \left[a - (a-b)\sin^2\theta\cos^2\psi\right]^2,$$

$$I_{A_1}^{VH} \sim \left[\frac{a-b}{2}\sin^2\theta\sin(2\psi)\right]^2,$$

where the light polarization angle ψ is measured from the plane defined by $\mathbf{k}$ and the trigonal axis c_3. For incidence along the trigonal axis ($\theta = 0$), only the parallel-polarizer configuration has nonzero intensity, independent of the polarization direction. The angular dependence is circular, with intensity proportional to a^2. As θ increases above zero, the circle elongates into an oval-like shape. The calculations give $b > a$ for α-GeTe, so the oval is elongated along the trigonal axis c_3. The angular intensity dependence of the E-modes is more complicated: in general, it varies with both the polar and azimuthal angles. For incidence along the trigonal axis ($\theta = 0$), it is a circle whose radius is determined by c. For incidence perpendicular to the trigonal axis ($\theta = 90^\circ$), the E-mode intensity has a four-lobed angular dependence. At small angles θ, the parallel and crossed polarization intensities can be approximated by

$$I_E^{VV} \approx c^2 - 2cd\theta\big(\sin(3\phi + 2\psi) + \sin(3\phi + 4\psi)\big),$$

$$I_E^{VH} \approx c^2 + 2cd\theta\sin(3\phi + 4\psi).$$

These expressions show that the circle may be distorted because the intensities depend on the sines of 2ψ and 4ψ. A detailed description of the calculation procedure for the E-modes and calculated angular intensity dependences of the E and A_1 phonon modes at 10° increments in the orientation angles of $\mathbf{k}$ will be presented in an extended publication.

For experimental investigation of the effect of structural anisotropy on the vibrational properties of α-GeTe, Raman intensity polar plots were measured and analyzed. In these measurements, the linearly polarized laser excitation first passed through a half-wave plate positioned before the focusing objective. Rotating the half-wave plate by a fixed angle rotated the incident-light polarization in the horizontal plane. Raman-scattered light from the sample was collected by the same objective and passed through the same half-wave plate. Its polarization vector was thus rotated by the same angle in the opposite direction. Rotating an analyzer before the entrance slit of the spectrometer enabled either the parallel or the crossed component of the polarized Raman spectrum to be recorded. The experimental setup is shown in Figure 1, *a*. This procedure ensured that the angular dependences of the phonon mode intensities were measured at the same sample location with micrometer accuracy.

TEM showed that the crystals have a domain structure, apparently formed during the phase transition from the high-temperature cubic β-GeTe phase with the NaCl structure to the rhombohedral α-GeTe phase. Figure 1, *b* and *c* shows electron diffraction patterns of the TEM sample regions subsequently investigated by μ-RS. Raman spectra were recorded from TEM specimen regions whose domain crystallographic orientations had first been established from electron diffraction patterns, allowing experimental and calculated angular dependences to be compared. Here we present results only for two experimental geometries with the greatest difference in the relative orientations of the light wave vector $\mathbf{k}$ and crystal trigonal axis c_3. The full set of angular Raman intensity dependences measured on different α-GeTe planes, together with a detailed analysis, will be presented in an extended publication.

Figure 2, *a* shows the Raman intensity polar plots of two phonon modes, E ($87\,\mathrm{cm}^{-1}$) and $A_1(\mathrm{LO})$ ($124\,\mathrm{cm}^{-1}$), measured in backscattering geometry with the incident and scattered wave vectors along the trigonal axis c_3. The calculated angular dependences for this experimental geometry are also shown. The calculated and experimental intensities of the $A_1(\mathrm{LO})$ mode agree very well in the parallel (VV) component of the polarized Raman spectrum, showing complete isotropy over $0-360^\circ$. The selection rules forbid the A_1 mode in the crossed (VH) component of the Raman spectrum. This condition is satisfied by both the calculated and experimental data. For the E mode, theory predicts complete isotropy in the VV and VH-components of the polarized Raman spectrum and similar intensities in the two components. The experimentally measured intensities of this mode in the two components are similar in magnitude, but their angular dependences are not fully isotropic. Modeling showed that these distortions can be explained by a slight misalignment of the sample surface normal with the trigonal axis.

Figure 2, *b* shows Raman intensity polar plots for the two phonon modes, E ($85\,\mathrm{cm}^{-1}$) and $A_1(\mathrm{TO})$ ($123\,\mathrm{cm}^{-1}$), measured in backscattering geometry with the incident and scattered wave vectors perpendicular to the trigonal axis c_3. Calculated angular dependences for this experimental geometry are also shown. The experimental and theoretical angular Raman intensity dependences agree very well for both the E and $A_1(\mathrm{TO})$ modes, revealing strong anisotropy. The E mode exhibits a pronounced, predominantly two-lobed pattern in the VV-component and a four-lobed pattern in the VH-component of the Raman spectrum. The intensity maxima in the VV- and VH-components are shifted by 45°. The $A_1(\mathrm{TO})$ mode exhibits a two-lobed pattern only in the VV-component. In the VH-component of the

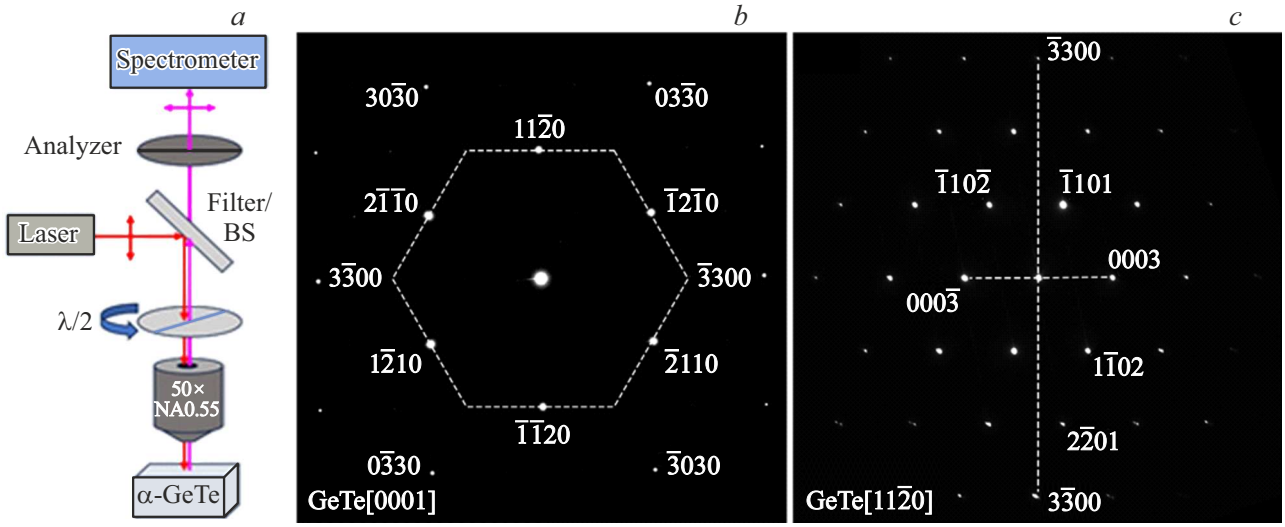


Figure 1. *a* — angle-resolved μ-RS experimental setup; *b* and *c* — electron diffraction patterns for the two α-GeTe crystal orientations on the TEM grid considered here: *b* — a crystal section close to the basal plane (0001); *c* — a section along a prismatic plane of type $\{11\bar{2}0\}$.

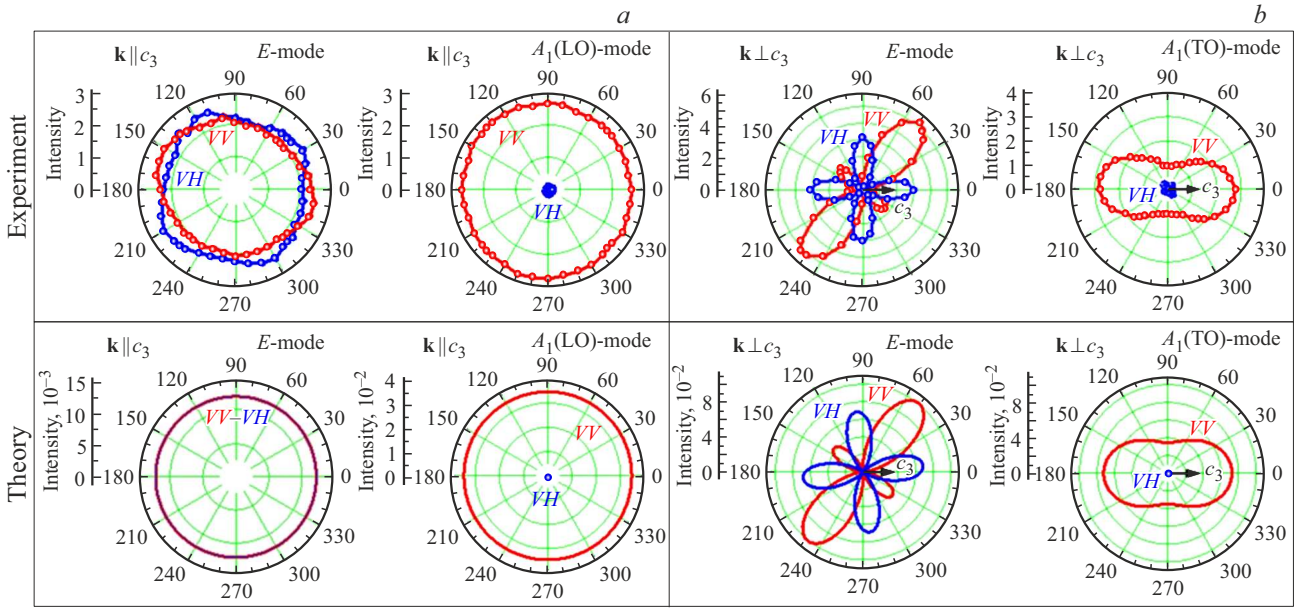


Figure 2. Experimental and theoretical polar plots of the intensities of phonon modes of symmetry E and A_1 in the Raman spectrum of α-GeTe. Experimental geometries: *a* — light wave vector **k** parallel to the trigonal axis c_3 (crystal section close to the basal plane (0001)); *b* — light wave vector **k** perpendicular to the trigonal axis c_3 (section along a prismatic plane of type $\{11\bar{2}0\}$).

polarized Raman spectrum, the A_1(TO) intensity is low because it depends on the difference between *a* and *b*. As noted above, the Raman spectra were collected from the same sample regions which crystallographic directions had been determined by analyzing electron diffraction patterns obtained via TEM. This allowed the intensity plot of the A_1(TO) mode in the *VV* component to be associated with the trigonal axis *c* (Figure 2, *b*). The experimentally determined trigonal-axis direction agrees fully with the theoretical prediction that the oval intensity plot of the A_1(TO) mode in α-GeTe is elongated along the trigonal axis.

Reference [10] first reported infrared PL from α-GeTe in the 0.7–0.8 eV range. Analysis of the experimental PL spectra as functions of carrier (hole) concentration and temperature, using the density functional electronic structure calculations reported in Ref. [10], indicates an interband origin. Here we investigated changes in the low-temperature ($T = 5$ K) PL spectra of the α-GeTe samples

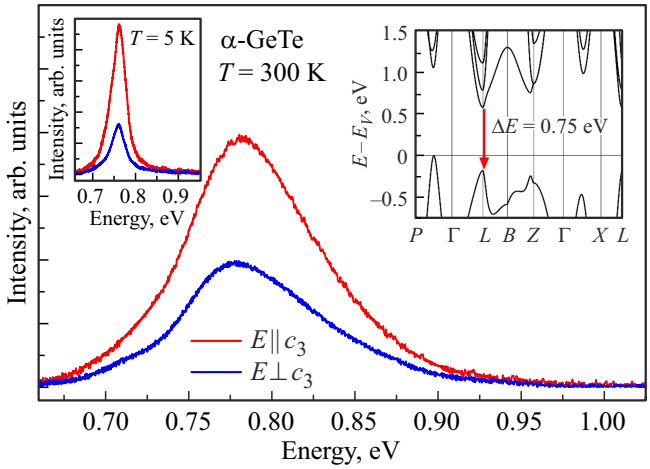


Figure 3. Polarized PL spectra of an α-GeTe sample measured on the $(11\bar{2}0)$ face at $T = 300$ and 5 K (left inset). The right inset shows the electronic band structure of α-GeTe calculated in this work.

as the excitation power was varied. The integrated PL intensity was found to depend almost linearly on excitation power over two orders of magnitude, as is characteristic of direct interband transitions. PL spectra were also measured using three excitation lasers spanning a broad energy range: 2.33 eV ($\lambda = 532$ nm), 1.95 eV ($\lambda = 633$ nm), and 0.94 eV ($\lambda = 1318$ nm). Approximately the same excitation power density at the sample was maintained for all three lasers. The PL spectral shape was found to depend on excitation power density but not on excitation photon energy. These results are also typical of direct interband transitions. Density functional electronic band structure calculations using VASP [11,12] support this conclusion. The direct gap between the conduction and valence bands at the L point of the BZ was 0.75 eV, consistent with the PL peak position and suggesting direct transitions between conduction and valence band states near the L point (Figure 3). A detailed description of the experimental and theoretical investigation of the origin of infrared PL in α-GeTe will be presented in an extended publication.

Using the trigonal-axis c_3 direction of α-GeTe determined from the Raman intensity polar plots, we measured the anisotropy of polarized PL. The room-temperature and cryogenic data shown in Figure 3 demonstrate that polarized PL is highly sensitive to the structural anisotropy of α-GeTe. At $T = 5$ K, the intensity of the PL polarized parallel to the trigonal axis c_3 was ~ 3 times higher than that polarized perpendicular to the axis. At 300 K, this ratio was close to 2 (Figure 3).

To summarize, a combined experimental and theoretical investigation of the angular dependences of phonon mode intensities in the Raman spectra of α-GeTe crystals was performed for the first time. Using the crystallographic directions determined by TEM in the α-GeTe samples, we compared the experimental and calculated angular dependences, which proved virtually identical. This enabled development of a rapid, nondestructive method for determining the crystallographic orientation of α-GeTe samples from Raman measurements. Because of the close relationship between structural anisotropy and the anisotropy of optical, electrical, and thermal properties, this result may advance understanding of the physical properties of α-GeTe. Strong anisotropy of interband PL ($\sim 0.7-0.8$ eV) in α-GeTe near the L point of the BZ was detected for the first time. At $T = 5$ K, the intensity of the PL polarized parallel to the trigonal axis c_3 of α-GeTe was ~ 3 times higher than that polarized perpendicular to c_3. At $T = 300$ K, the ratio was close to 2.

Funding

This work was supported in part by Russian Science Foundation grant №25-42-00053, https://rscf.ru/project/25-42-00053/

Conflict of interest

The authors declare that they have no conflict of interest.

References

[1] A.V. Kolobov, P.I. Lazarenko. Semiconductors, **59**, 469 (2025). DOI: 10.61011/SC.2025.09.62832.8784

[2] Y. Yu, X. Xu, M. Bosman, K. Nielsch, J. He. Nature Rev. Electr. Eng., **1**, 109 (2024). DOI: 10.1038/s44287-023-00013-6

[3] M. Li, X.L. Shi, Z.G. Chen. Adv. Funct. Mater., **34**, 2403498 (2024). DOI: 10.1002/adfm.202403498

[4] S. Yang, F. Sui, Y. Liu, R. Qi, X. Feng, S. Dong, P. Yang, F. Yue. Nanoscale, **15**, 13297 (2023). DOI: 10.1039/d3nr02678g

[5] H. Chen, Q. Song, Z. Zhang, S. Wan, L. Chen, S. Bai. J. Mater. Chem. A, **12**, 10974 (2024). DOI: 10.1039/d4ta01087f

[6] E.F. Steigmeier, G. Harbeke. Solid State Commun., **8**, 1275 (1970). DOI: 10.1016/0038-1098(70)90619-8

[7] R. Loudon. Adv. Phys., **13**, 423 (1964). DOI: 10.1080/00018736400101051

[8] X. Gonze, B. Amadon, G. Antonius, F. Arnardi, L. Baguet, J.-M. Beuken, J. Bieder, F. Bottin, J. Bouchet, E. Bousquet, N. Brouwer, F. Bruneval, G. Brunin, T. Cavignas, J.-B. Charraud et al. Comput. Phys. Commun., **248**, 107042 (2020). DOI: 10.1016/j.cpc.2019.107042

[9] X. Gonze, Ch. Lee. Phys. Rev. B, **55**, 10355 (1997). DOI: 10.1103/PhysRevB.55.10355

[10] V.Yu. Davydov, A.N. Smirnov, I.A. Eliseyev, M.K. Sakhno, A.V. Myasoedov, D.A. Pshenay-Severin, A.A. Shabaldin, A.T. Burkov. Fiz. Tverd. Tela, **67**, 2446 (2025). DOI: 10.61011/FTT.2025.12.62446.7970k-25 (In Russian).

[11] G. Kresse, J. Furthmuller. Phys. Rev. B, **54**, 11169 (1996). DOI: 10.1103/PhysRevB.54.11169

[12] G. Kresse, D. Joubert. Phys. Rev. B, **59**, 1758 (1999). DOI: 10.1103/PhysRevB.59.1758